Proceedings of the
1999 ASME Design Engineering Technical Conferences
September 12-15, 1999, Las Vegas, Nevada

DETC99/VIB-8211

COMMAND PREPROCESSOR FOR RADIOTELESCOPES AND MICROWAVE ANTENNAS

Wodek Gawronski
Jet Propulsion Laboratory, California Institute of Technology, Pasadena, CA 91109

ABSTRACT

The LQG controllers, designed for the NASA Deep Space Network antennas have small tracking errors and are resistant to wind disturbances. However, during antenna slewing, they induce limit cycling caused by the violation of the antenna rate and acceleration limits. This problem can be avoided by introduction of a command that does not exceed the limits. The command preprocessor presented in this paper generates a command that is equal to the original command if the latter does not exceed the limits, and varies with the maximal (or minimal) allowable rate and acceleration if the limits are met or exceeded. It is comparatively simple since it requires only knowledge of the command at the current and the previous time instants, while other known preprocessors require knowledge of the terminal state and the acquisition time. Thus, the presented preprocessor is more suitable for implementation. In this article analysis of the preprocessor is presented. Also the performances of the preprocessor itself, and of the antenna with the preprocessor is illustrated with typical antenna commands.

INTRODUCTION

Radio-telescopes [1], and microwave antennas [2] are flexible multi-body systems. An example of the NASA/JPL beam-wave guide antenna with 34-meter dish is shown in Fig.1. The antenna can rotate with respect to the azimuth (vertical) and elevation (horizontal) axes. These antennas are equipped with precision tracking controllers. However, their implementation is limited due to antenna limit cycling during slewing operations, as reported in Ref.[3]. The limit cycling is due to the non-linear dynamics imposed by antenna rate and acceleration limits. In order to avoid the cycling, one can either apply gain scheduling (different controller gains for tracking and for slewing) or use a command preprocessor (CPP). The preprocessor is computer software that generates a modified command, identical with the original one, if the rate and accelerations are within the limits and a command of maximal (or minimal) rate and acceleration when the limits are met or violated.

A preprocessor algorithm was developed by Tyler [4]. In order to generate a modified trajectory, this algorithm requires advance knowledge of the final state (i.e., position and rate) of the antenna, and the time required to reach the final state. In many cases the final state is not known (for example, in the case of acquiring a moving target), and the time of acquisition cannot be precisely determined. Thus two requirements - the knowledge of the acquisition state and time - make this algorithm useful in selected applications only. The algorithm proposed below does not require the knowledge of the above parameters. It determines the preprocessed command based on the current and previous value of the original command. The basic idea of this preprocessor was previously described in [5].

CPP DESCRIPTION

The block diagram of the CPP is shown in Fig.2. Its main line of the block diagram consists of a derivative, an integrator, and rate and acceleration limiters. The proportional feedback loop has variable gain k_i; the gain depends on the preprocessor error e_i. The sampling time is denoted T (where T=0.02 s); the command at the ith time instant $t = iT$ is denoted r_i; the command rate is v_i; the preprocessed command is denoted r_{pi}; the input to the integrator is u_i; and the preprocessor error is $e_i = r_i - r_{pi}$.

Consider a case where the command r_i does not exceed the rate and acceleration limits. In this case the system is linear, and the rate and acceleration limiters in Fig.2 are replaced with a unit gain. For the linear case the equations are:

- for the integrator:

$$r_{pi} = r_{pi-1} + Tu_i \tag{1a}$$

- for the derivative

$$v_i = \frac{r_i - r_{i-1}}{T} \tag{1b}$$

- for the error

$$e_i = r_i - r_{pi} \tag{1c}$$

- and for the integrator input

$$u_i = k_i e_{i-1} + v_i \tag{1d}$$

Combining the above equations, one obtains

$$r_{pi} - r_{pi-1} + Tk_i r_{pi-1} = r_i - r_{i-1} + Tk_i r_{i-1} \tag{2}$$

The above equation shows that $r_i = r_{pi}$ for zero initial conditions. In consequence, if the preprocessed command reaches the original command, it follows exactly the latter one.

The transient motion of CPP has to be investigated. In order to do this, the equation (2) can be re-written as

$$e_i = \alpha_i e_{i-1} \tag{3a}$$

where

$$\alpha_i = 1 - Tk_i. \tag{3b}$$

This is an equation of the transient dynamics of the CPP error. From (3a) it follows that the system is stable if $|\alpha_i| < 1$. For $0 < \alpha_i < 1$ there is no overshoot, and for $-1 < \alpha_i < 0$ the transient is oscillatory, $i = 1,2,\ldots$. Consider further only positive α_i, the case with no overshoot of the preprocessed command over the original command. Note in this case that the smaller the gain α_i is, the quicker the error dies down. The gain k_i controls the value of α_i, see (3b); therefore for large-gain k_i the transient between the original and the preprocessed command is strongly damped.

However, too large of a gain may cause the violation of the rate and/or acceleration limits, which, in turn, causes non-linear behavior and increases the error. In order to avoid this situation the variable gain is introduced. It depends on the error e_i. The gain is large for small error, and smaller for large error. It is assumed in the form:

$$k_i = k_o + k_v e^{-\beta|e_i|} \tag{4}$$

where k_o is the constant part of the gain, k_v is the variable part of the gain, and β is the gain exponential. The plot of $k_i(e_i)$ for $k_o = 1$, $k_v = 5$, and for $\beta = 10, 20, 40,$ and 100 is shown in Fig.3. From this figure one can see that, for a small error, gain reaches its maximal value, and for the large error, the gain is minimal.

Step inputs are used as a mean of determination of the variable gain parameters. For the antenna sampling time $T = 0.02$ s and the rate limit v_{max} =0.8 deg/s, the maximal step that does not violate the rate limit is $v_{\max} T = 0.016$ deg. On the other hand our measurements show that the step responses above 0.15 deg show non-linear behavior. The gain k_o, the lower value of k_i, was assumed 1, in order to perform properly for small steps of 0.016 deg or smaller. The upper value of the variable gain, $k_o + k_v$, is assumed 6 for the acceptable performance at large steps, of 0.15 deg or larger. This process is illustrated later. For the error within the interval [0.016 0.150] deg the gain varies from its maximal to its minimal value. The exponential constant β defines this gain variation. We have chosen $\beta = 20$ since for this value the gain changes from its maximal to minimal value within the segment of [0.016, 0.150] deg.

The nonlinear behavior of the CPP mimics the antenna nonlinear dynamics. Namely, in the Fig.2, the integrator is a model of an ideal (or rigid) antenna, the derivative represents the antenna feed-forward gain (that perfectly inverses the rigid antenna model), the gain k_i represents the antenna controller, and the rate and acceleration limiters are located at places corresponding to the antenna locations. In this way, the non-linear dynamics of CPP is close to the desirable dynamics of an antenna.

CPP DYNAMICS

The CPP dynamics is checked in the three scenarios, typical for the DSN antennas:

(1) Step responses, both small and large. Small steps do not violate the limits; large steps do.
(2) Rate offsets.
(3) Acquiring and tracking a typical trajectory.

We will consider also two types of CPP:

(1) With constant gain, that is $k_i = 1$ for all i.

(2) With variable gain, as in (4), with $k_o = 1$, $k_v = 5$, and $\beta = 20$.

The rate and acceleration limits of the antenna are 0.8 deg/s and 0.4 deg/s^2, respectively, and the rate and acceleration limits of the CPP were of 90 percent of the antenna limits.

For the large step of 10 deg the preprocessed command, its rate and acceleration are shown in Fig.4a-c (for the constant gain CPP), and in Fig.4d-f (for the variable gain CPP). The figure shows little difference between the preprocessed command with constant gain CPP and with the variable gain CPP. Both preprocessed commands begin with the maximal acceleration until they reach the maximum rate, then continue with the maximal (and constant) rate and finally slow-down with the minimal deceleration. After reaching the steady-state value of 10 deg the error between the original and the preprocessed command is zero.

For a small step of 0.01 deg the preprocessed command, its rate, and acceleration are shown in Fig.5a-c (for the constant gain CPP), and in Fig.5d-f (for the variable gain CPP). The figure shows a significant difference between the preprocessed commands with constant and variable gain. Comparatively low constant gain ($k_o = 1$) results in the slow response of the CPP, namely 6 s settling time. The variable gain CPP generates a command with 1 s settling time due to the high gain value for the small error. The settling time is an important factor when the antenna dynamics is considered, see the next section.

A rate offset was simulated and is shown in Fig.6. The preprocessed commands (for the constant and variable gain CPP) are almost the same. Small differences are in the rate and acceleration profiles.

Finally, a typical azimuth trajectory acquiring and tracking by the CPP is shown in Fig.7a. The antenna position at the initial time is 14 deg, while the target position is at 24 deg. The target is acquired in 15 s with the maximal speed (see Fig.7b) and maximal acceleration (see Fig.7c), and also with very small overshoot (c.f. Fig7a). The CPP error (the difference between the original and preprocessed trajectory) after the acquiring is virtually zero.

ANTENNA DYNAMICS

The antenna rotates with respect to AZ and EL axes. The antenna dynamics with respect to these axes is decoupled. The cross-coupling (AZ-EL and EL-AZ) is less than 0.1 percent of the straight coupling (AZ-AZ and EL-EL). For this reason the AZ and EL dynamics is analyzed separately. For the sake of space savings we present the AZ dynamics only.

The azimuth model is obtained from the field data collected at the DSS54 antenna at Madrid, Spain. The magnitude and phase of the transfer function identified from the data are shown in Fig.8a,b. The plots show that the open-loop antenna model is an integrator for low frequencies, and inherits a flexible structure properties (resonances) for higher frequencies.

For this model an LQG controller was designed. The block diagram of the controller is shown in Fig.9. The controller is divided into the PI part, responsible for the tracking properties, and into flexible mode part, responsible for the damping of flexible motion. This controller was tested at the antenna, obtaining step response as in Fig.10a. The rate and acceleration of the antenna are shown in Fig.10b,c, respectively. Both are within the imposed limits (0.8 deg/s and 0.4 deg/s^2). For large steps, however, the antenna hits rate and acceleration limits (see Figs.11b,c) which causes limit cycling.

DYNAMICS OF THE ANTENNA WITH CPP

In this section the dynamics of the antenna with the constant and variable CPP are presented. The following simulations show that the presented CPP prevents the cycling.

The response of the constant gain CPP to the small step input of 0.01 deg is shown in Fig.12a dashed line. It is a slow response of 6 s, with no overshoot. In this case the antenna follows closely the preprocessed command. The response of the variable gain CPP to the small step input is shown in Fig.12b. It is a rapid response of less than 1 s. The antenna follows the preprocessed command with the overshoot. This response is similar to its response to the non-processed step of 0.01 deg.

The responses of the constant and variable gain CPP to a large step input of 10 deg is shown in Fig.13a dashed line and the antenna responses in solid line. Both are practically identical, and have no overshoot. For comparison, the response of the same antenna to non-processed step is shown in Fig.11a. Clearly, limit cycling similar to the one previously observed during the antenna controller tests is visible.

The antenna responses to the preprocessed rate offset, and to the preprocessed azimuth trajectory can be separated into two segments: a linear one (where the original command does not exceed the rate and/or acceleration limits) and non-linear one (where it does). Within the nonlinear segment the antenna response is very close to the preprocessed command, and in the linear segment the antenna response was identical to the response to the original command. This is illustrated in Fig.14 with the antenna response to the preprocessed azimuth trajectory as in Fig.7a. In 15 s, the antenna acquires the original trajectory, since it follows very closely the preprocessed trajectory. In Figs.14a,b the preprocessed trajectory is denoted

with dashed line, and the antenna response with solid line; both lines overlap.

CONCLUSIONS

The proposed CPP is a computer algorithm that processes the antenna commands. The processed command is identical to the original one if the latter does not exceed the antenna rate and acceleration limits. If the limits are exceeded, the preprocessed command variations are subject to the maximal or minimal rates and accelerations. The proposed preprocessor algorithm is simple since it does not require knowledge of future antenna positions. Rather, it uses the current and previous values of the original command. The simulation results show that the CPP commands make the LQG controllers stable in slewing and accurate in tracking.

REFERENCES

[1] W. Gawronski, and B. Parvin, "Modeling and Analysis of the Green Bank Telescope Control System," *NRAO Green Bank Telescope Memo*, No. 129, April 1995.

[2] W. Gawronski, and J.A. Mellstrom, "Control and Dynamics of the Deep Space Network Antennas," in: *Control and Dynamics Systems*, ed. C.T. Leondes, vol. 63, Academic Press, San Diego, CA, 1994, pp. 289-412.

[3] W. Gawronski, H.G. Ahlstrom, Jr., and A.B. Bernardo, "Design and Performance of the DSS-14 Antenna Controller," *The Telecommunications Mission Operations Progress Report 42-135, July-September 1998,* Jet Propulsion Laboratory, Pasadena, California, November 15, 1998.

[4] S.R. Tyler, "A Trajectory Preprocessor for Antenna Pointing," *The Telecommunications and Data Acquisition Progress Report 42-118, April-June 1994*, August 15, 1994.

[5] W.K. Gawronski, C.S. Racho, and J.A. Mellstrom, "Application of the LQG and Feedforward Controllers to the Deep Space Network Antennas," *IEEE Transactions on Control System Technology,* vol.3, No.4, Dec. 1995, pp.417-421.

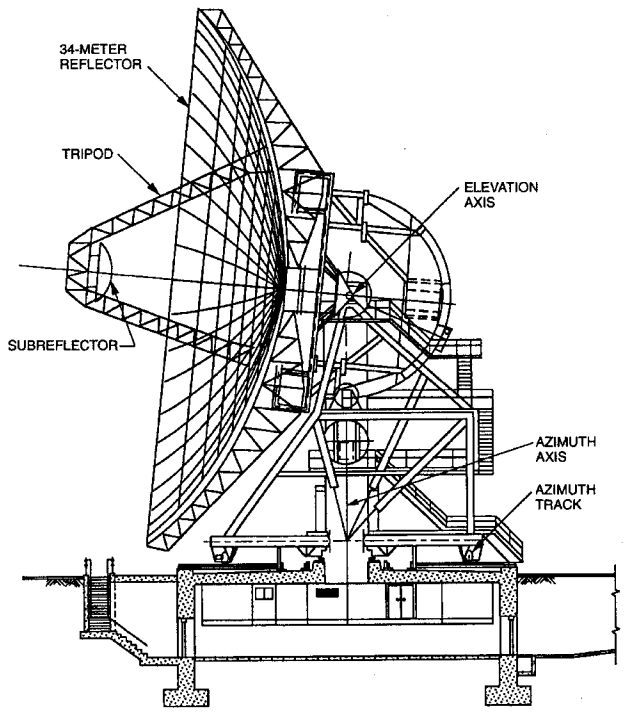

Figure 1. The Deep Space Network antenna.

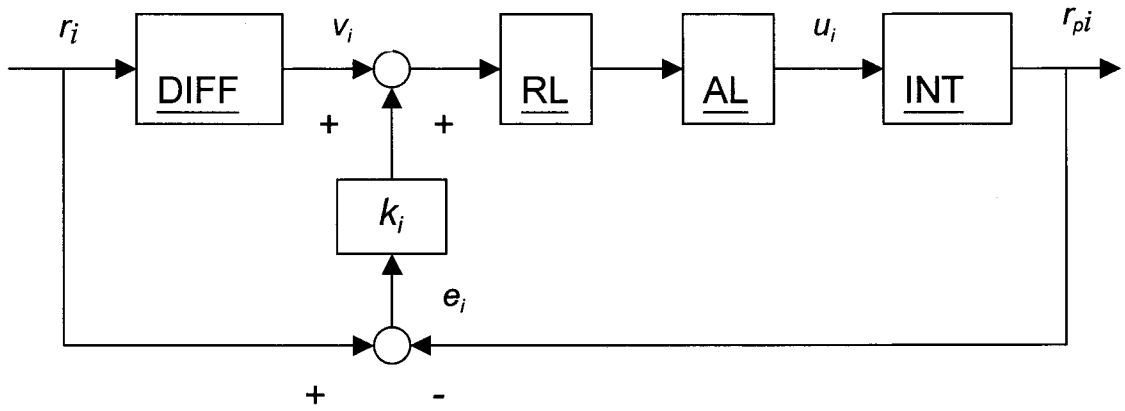

Figure 2. The command preprocessor

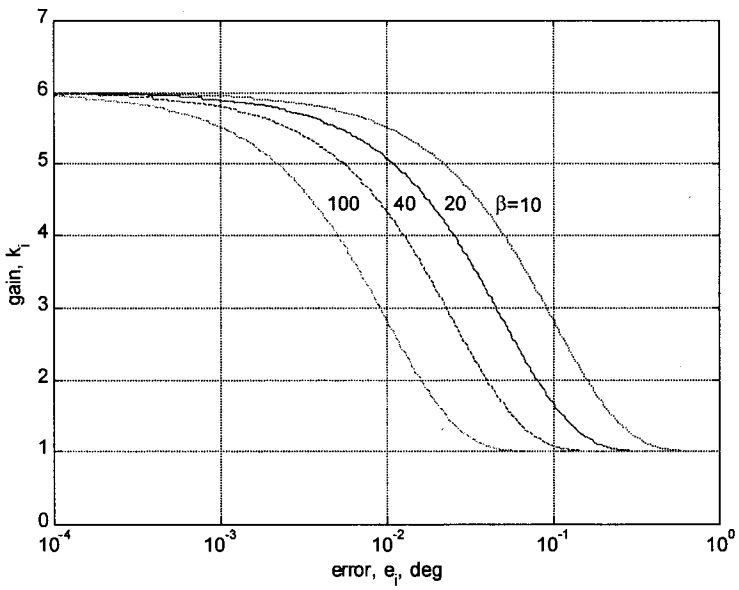

Figure 3. The CPP gain versus the CPP error

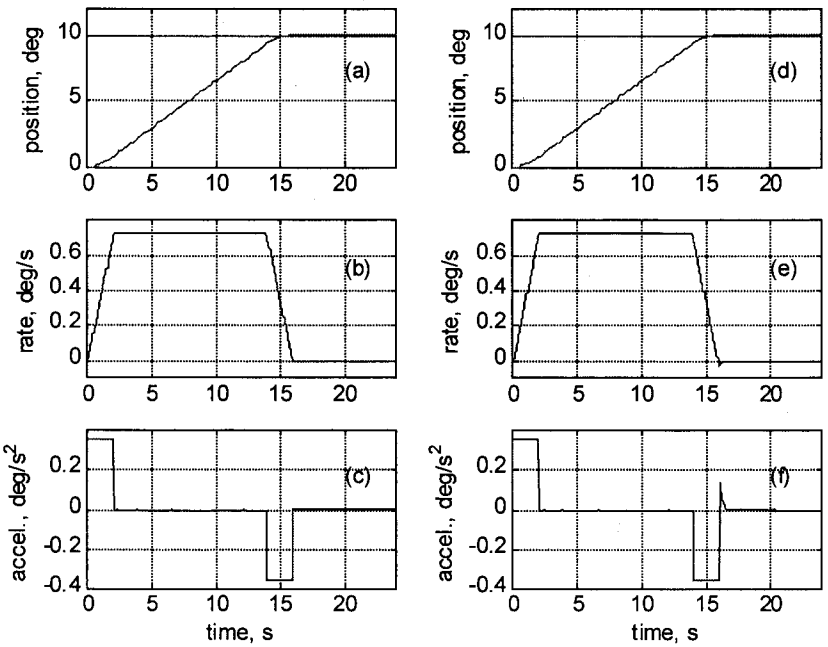

Figure 4. The preprocessed large-step commands for the constant-gain CPP (a) command, (b) rate, and (c) acceleration, and for the variable-gain CPP (d) command, (e) rate, and (f) acceleration

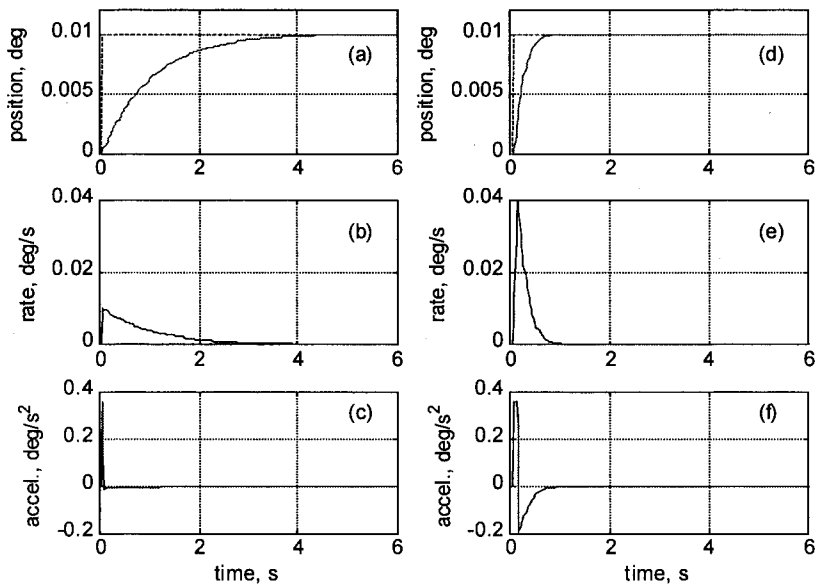

Figure 5. The preprocessed small-step commands for the constant-gain CPP (a) command, (b) rate, and (c) acceleration, and for the variable-gain CPP (d) command, (e) rate, and (f) acceleration

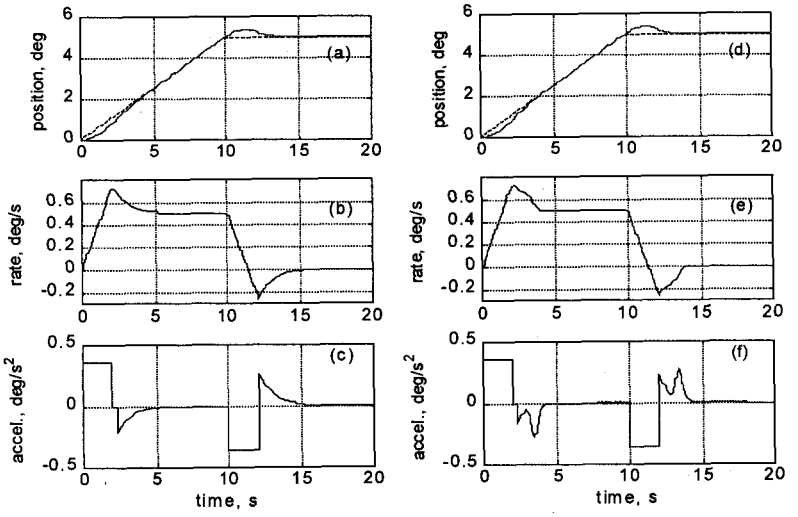

Figure 6. The original and preprocessed rate offsets for the constant-gain CPP (a) command, (b) rate, and (c) acceleration, and for the variable-gain CPP (d) command, (e) rate, and (f) acceleration

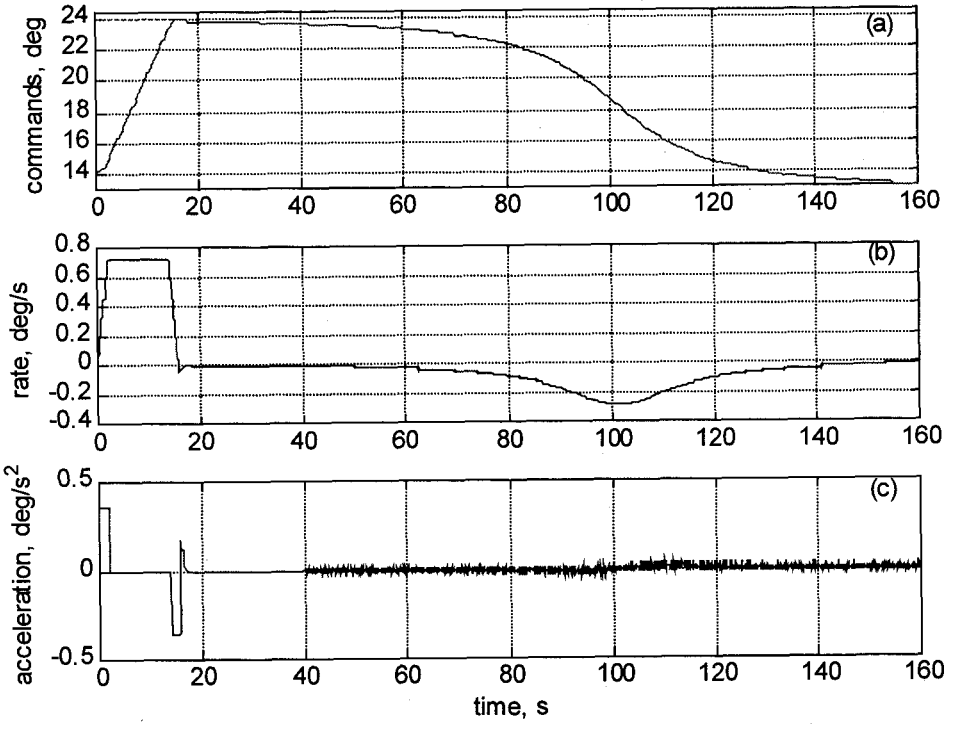

Figure 7. The original and preprocessed azimuth trajectory: (a) command, (b) rate, and (c) acceleration

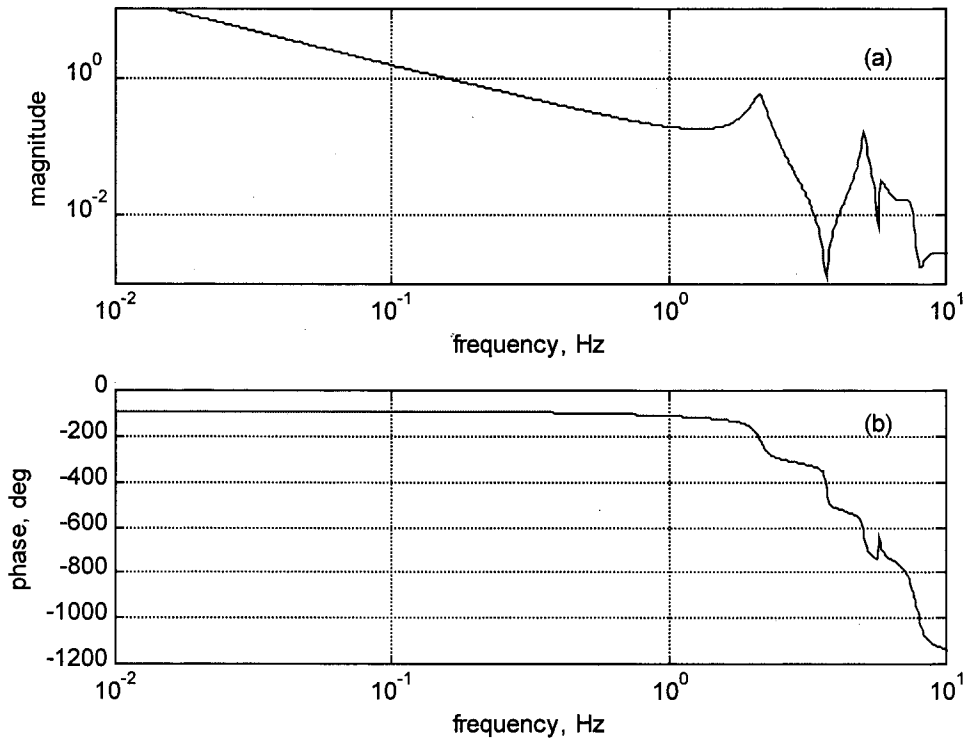

Figure 8. Transfer function of the open-loop antenna, (a) magnitude, (b) phase.

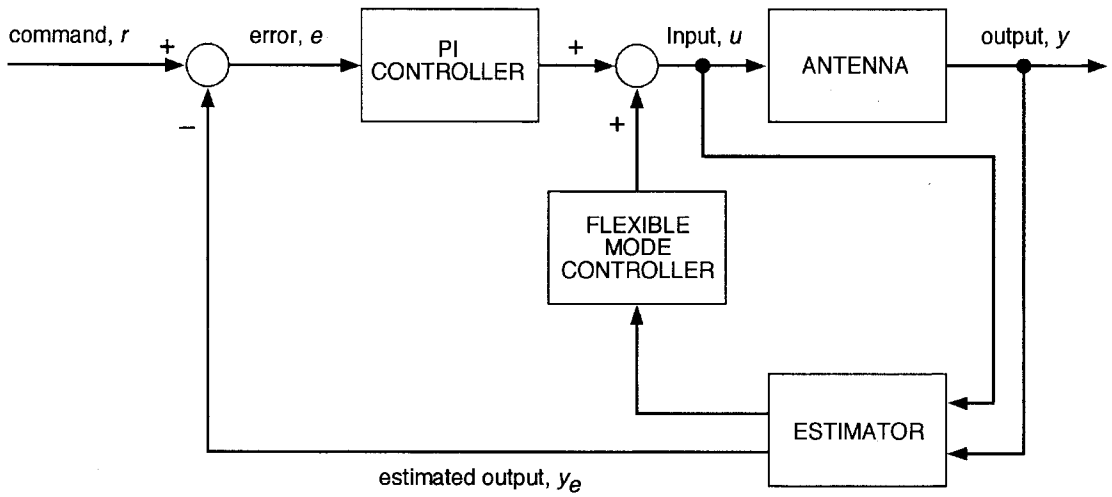

Figure 9. LQG controller of the DSN antenna

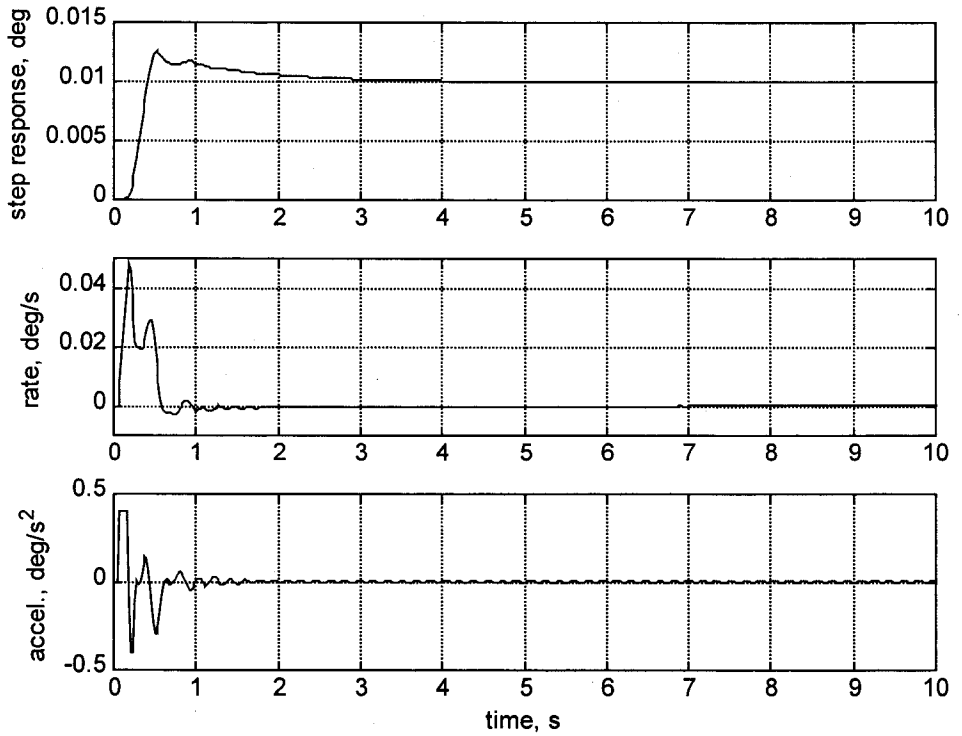

Figure 10. Small step response of the closed-loop antenna (a) position, (b) rate, and (c) acceleration

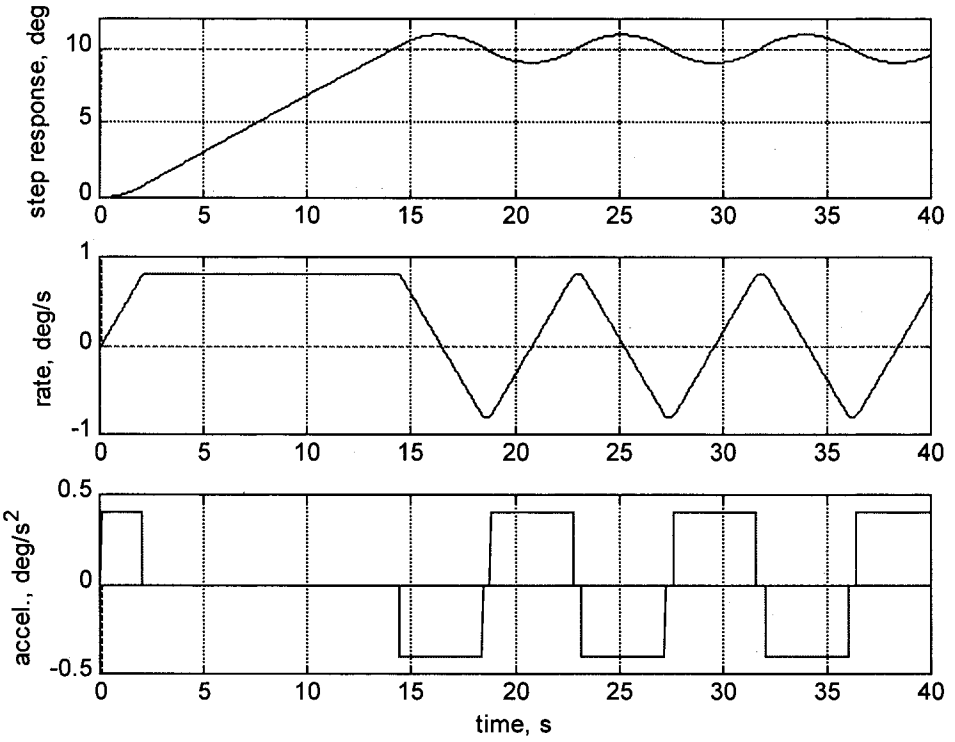

Figure 11. Large step response of the closed-loop antenna (a) position, (b) rate, and (c) acceleration

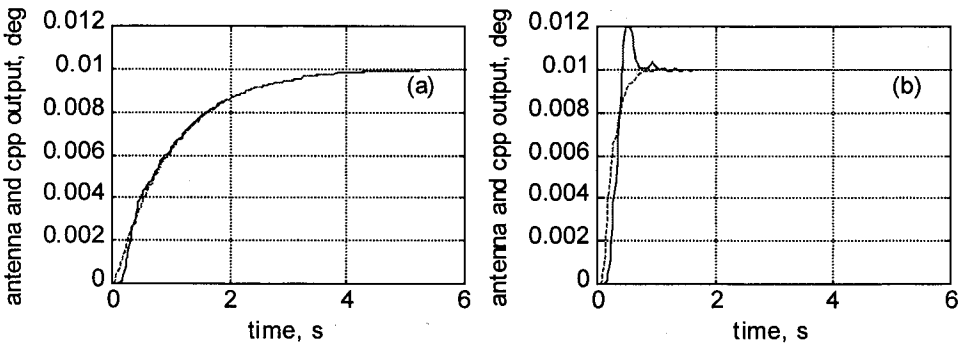

Figure 12. The antenna response to the preprocessed steps for the (a) constant-gain CPP and (b) variable-gain CPP.

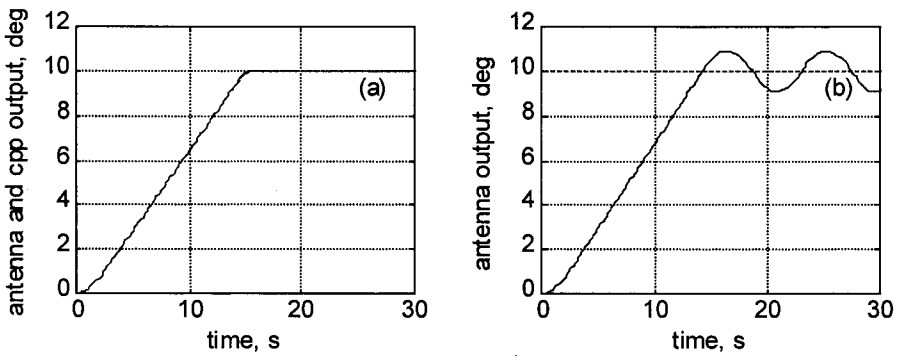

Figure 13. The antenna response to the preprocessed large steps for the (a) preprocessed step and (b) original step.

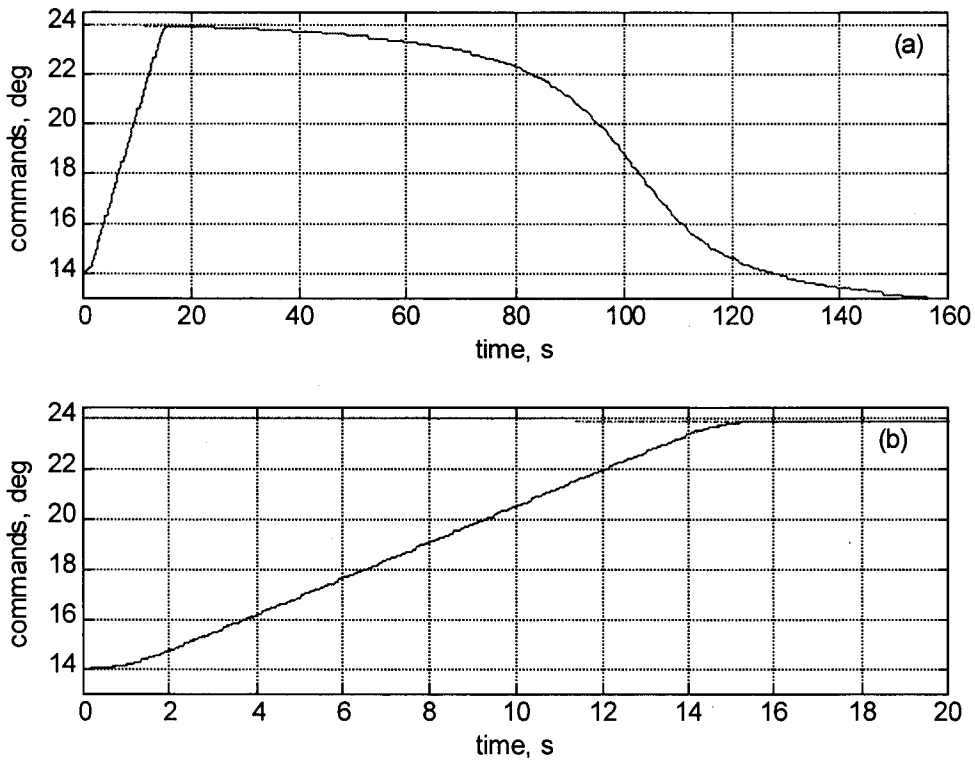

Figure 14. Azimuth tracking of the preprocessed command (a) original trajectory and (b) acquisition segment